TEMPERATURE-PROGRAMMED PYROLYSIS OF $(NH_4)_2Cr_2O_7$-MODIFIED CELLULOSIC MATERIALS

I.Y. Petrov, E.S. Kotlyarova, and B.G. Tryasunov[*]
Institute of Coal and Coal Chemistry, SB RAS, 18 Sovetsky Ave., Kemerovo 650099, Russia
[*] *Kuzbass State Technical University, 28 Vessennyaya St., Kemerovo 650026, Russia*

Introduction

Pyrolysis of cellulosic materials is one of the traditional and widely used methods for producing various carbon adsorbents and catalyst supports [1]. However this process is associated with considerable losses in carbon (in form of volatile and/or tar-like products) and is characterized by relatively low char yields. The production of char is enhanced by low pyrolysis temperatures with slow heating rates, and higher pressures [2,3], but exact synthetic processes leading to char formation as well as the structure of the char still remain unknown. Some increase in char yield can be reached by decomposing cellulosic materials in the presence of inorganic acids [4], bases [5], metal chlorides [6] or ammonium salts [7]. Unfortunately, systematic studies on catalytic effects of different inorganic additives on the cellulose pyrolytic degradation were not still practically performed. Previously [8] the influence of Mo (VI), V (V), W (VI), B (III) and K (I) additives on carbonization of viscose fibers has been investigated. It has been shown that efficiency of the above dopants in charring reactions decreases in parallel with the drop in their acidity properties (estimated from the electronegativity values of these ions), excepting W (VI) species characterized by decreased dehydration activity at low temperatures of pyrolysis.

In the present work temperature-programmed pyrolysis combined with simultaneous continuous chromatographic analysis of gaseous products (H_2O, CO_2, CO) evolved in the range 20 ÷550^{o}C has been employed to study thermal transformations of some $(NH_4)_2Cr_2O_7$-doped cellulosic materials during their carbonization.

Experimental

$(NH_4)_2Cr_2O_7$-containing cellulosic samples were prepared by dry impregnation (series DI) or equilibrium adsorption (series EA) of microcrystalline cellulose (MCC) powder with aqueous solutions of ammonium dichromate, followed by drying of the supported materials at 110^{o}C for 4 h. In the case of the DI samples, the impregnating solutions were prepared with calculated amounts of $(NH_4)_2Cr_2O_7$ to obtain the required chromium concentration immediately after drying of the MCCs. The EA samples were prepared by soaking MCC into the aqueous solutions containing different amounts of $(NH_4)_2Cr_2O_7$ (250 ml; 0.0005-0.5 M). The preparations in Erlenmeyer flasks were agitated on a mechanical shaker for periods of up to 24 h before filtering and determining the final chromium contents. The chromium contents in the EA samples were determined spectrocolorimetrically by difference between optical densities of the fresh and used ammonium dichromate impregnating solutions. These measurements were made with a spectrocolorimeter Spekol-220 (Carl Zeiss Jena, Germany) at λ = 430 nm.

Temperature-programmed pyrolysis of cellulosic materials was carried out with the apparatus assembled on the base of a conventional gas chromatograph ("Tsvet-100", Russia), which was equipped with a standard pyrolytic attachment [9]. This method is based on the principle of sequential removing of separate constituents from a gas mixture (by their condensation or trapping with selective adsorbents), followed by analysis of residual gas flows after each step of the component elimination. A schematic view of the temperature-programmed pyrolysis setup is depicted in Fig. 1. The samples (5 mg) placed into a quartz reactor were pyrolyzed in a flow of He (25 ml/min) in the range 20-550^{o}C with a linear heating rate of 10^{o}C/min. H_2O, CO_2 and CO were the main gaseous pyrolysis products.

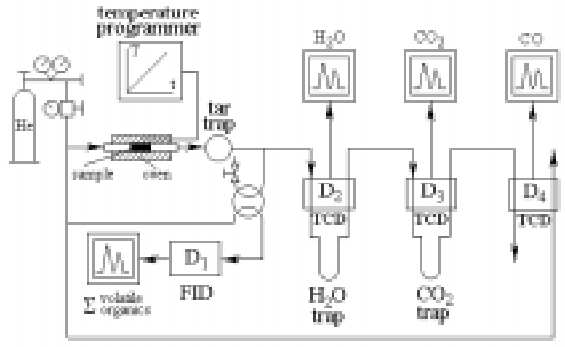

Figure 1. Schematic diagram of the setup for continuous analysis of cellulose pyrolysis gaseous products: TCD – thermal conductivity detector; FID – flame ionization detector.

Char yield measurements were performed using the same temperature-programmed setup (as in the case of temperature-programmed pyrolytic experiments). These experiments were carried out at the same operating conditions but with sample charges of ~ 15-16 mg. Char yields were calculated on the dmmf (dry mineral mattrer-free) base as weight percentages of coke formed during heating of modified cellulose samples up to 550^{o}C. The additive contents (as corresponding oxides formed from the precursor salts at 550^{o}C in inert medium) were subtracted from the total char yields.

X-ray diffraction (XRD) patterns of the samples were obtained with a "DRON-2.0" instrument (Nauchpribor, Russia) using Ni-filtered CuK_{α}-radiation. The crystallinity index (*CI*) of the original MCC and MCCs modified with ammonium dichromate were calculated from the wide angle X-ray diffractograms.by the Segal method described in [10].

The identification of the phases and structures formed in the course of the pyrolytic experiments was carried out by comparison of the XRD results obtained with the known literature data [10,11].

Results and Discussion

The results obtained are presented in Figures 2-3 and in Tables 1-2. X-ray diffraction patterns of pure MCC and $(NH_4)_2Cr_2O_7$-modified samples shows intense reflections at θ = 8.3, 11.3 and 17.3^{o} (Figs. 2and 3) are characteristic lines of cellulose I crystal structure. With chromium increasing, the relative intensity (per 1g of MCC) of these lines, as well as the crystallinity index of MCCs (Fig. 4.), tends to decrease. This data points out that some interaction of supported chromium species with cellulose crystalline structure occurs during the impregnation process.

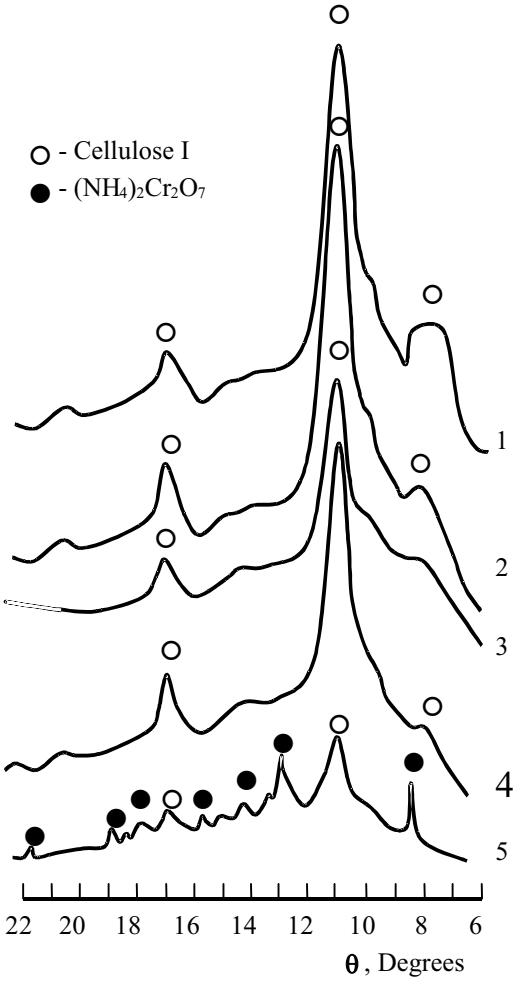

Figure 2. XRD patterns of the EA samples.

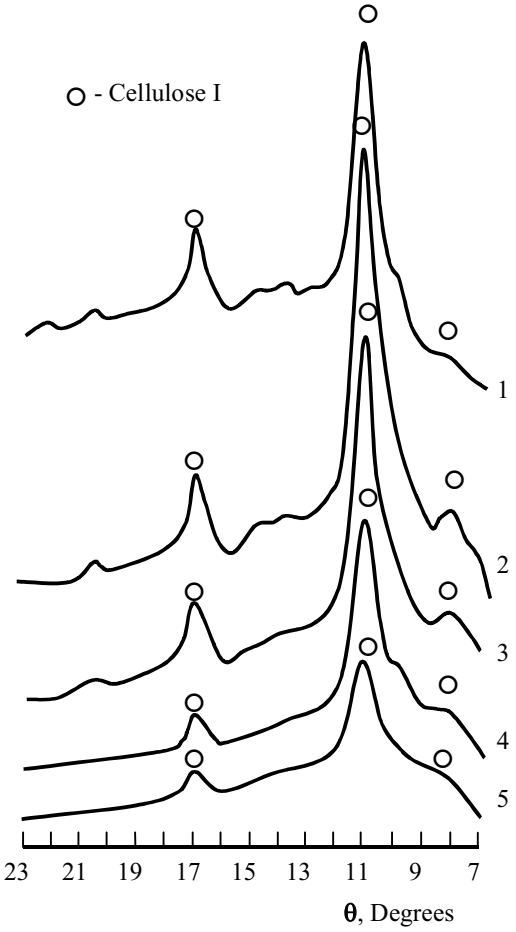

Figure 3. XRD patterns of the DI samples.

Table 1. Peak maximum temperature shifts and relative yields of gaseous products evolved during temperature-programmed pyrolysis of some DI samples

Sample	Chromium content $\cdot 10^4$ (moles Cr /1 g MCC)	Peak maximum temperature shift, ΔT (^{o}C)			Relative yield of gaseous products (a.u.)		$\frac{H_2O}{H_2O + CO + CO_2}$	Char yield
		H_2O	CO_2	CO	H_2O	$CO + CO_2$	(a.u.)	(%)
MCC	0.00	0.00	0.00	0.00	1.00	1.00	1.00	6.2
DI-1	$2.27 \cdot 10^{-1}$	15	15	20	0.84	0.78	1.03	8.0
DI-2	$4.54 \cdot 10^{-1}$	25	20	25	0.96	0.97	0.98	4.4
DI-3	3.64	30	35;–45	35;–40	1.82	1.84	1.00	18.8
DI-4	7.27	55	50;–35	45;–80	2.91	2.80	1.02	23.3
DI-5	14.54	50	45;–75	50;–120	2.65	3.41	0.90	n.d.*

* Not determined

Table 2. Peak maximum temperature shifts and relative yields of gaseous products evolved during temperature-programmed pyrolysis of some EA samples

Sample	Chromium content $\cdot 10^4$ (moles Cr /1 g MCC)	Peak maximum temperature shift, ΔT (^{o}C)			Relative yield of gaseous products (a.u.)		$\frac{H_2O}{H_2O + CO + CO_2}$	Char yield
		H_2O	CO_2	CO	H_2O	$CO + CO_2$	(a.u.)	(%)
MCC	0.00	0.00	0.00	0.00	1.00	1.00	1.00	4.0
EA-1	$2.20 \cdot 10^{-2}$	–10	–15	–20	0.85	0.76	1.05	3.6
EA-2	$1.07 \cdot 10^{-1}$	–5	–5	–10	0.95	0.94	1.00	5.3
EA-3	1.39	25	25;–120	25;–130	1.10	0.89	1.09	8.2
EA-4	2.92	25	20;–60	10;–50	2.76	2.55	1.03	17.6
EA-5	9.12	15	5;–25	5;–40	2.19	1.88	1.07	12.4

No additional lines are appeared up to the highest chromium contents. Only in the XRD pattern of the EA sample with $3.03 \cdot 10^{-3}$ M Cr/1g MCC several lines at θ = 8.9, 13.4, 14.8, 16.21, 18.38 and 22.21^o belonging to crystalline ammonium dichromate phase are observed (Fig. 2.).

All dry-impregnated samples have shown low temperature shifts ($\Delta T \sim +15 \div +50^oC$) of H_2O, CO_2 and CO evolution peaks relative to their position for pure microcrystalline cellulose (Table 1). Maximum temperatures of these peaks lowered with increasing the chromium content. The EA samples containing $<1.39 \cdot 10^{-4}$ M Cr/1g MCC have exhibited high temperature shifts of the above peaks ($\Delta T \sim -5 \div -20^oC$); however, at chromium contents $\geq 1.39 \cdot 10^{-4}$ M Cr/1g MCC, the thermal behavior of the EA cellulosics was similar to that of the DI samples (Table 2).

Irrespective of the preparation method, all low-concentrated samples ($<1.39 \div 3.64 \cdot 10^{-4}$ M Cr/1g MCC) were characterized by decreased yields of H_2O and CO_x (compared to pure cellulose). High-concentrated cellulosic materials ($>1.39 \cdot 10^{-4}$ M Cr/1g MCC), on the contrary, have shown the increased yields of the same products (cf. Tables 1 and 2).

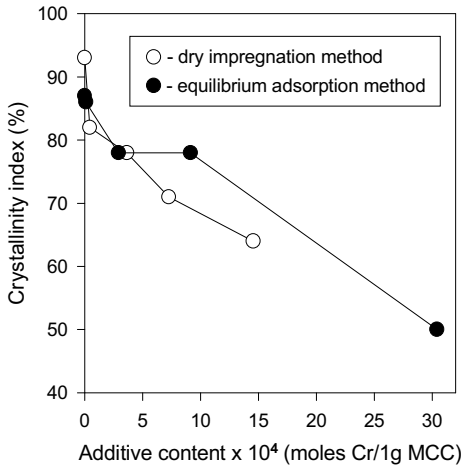

Figure 4. Variations in crystallinity indices of $(NH_4)_2Cr_2O_7$-doped MCCs with chromium content.

Also, in the case of chromium-rich cellulosics, at least two steps of CO_x evolution were observed (in contrast to one-stage elimination of CO_x for pure cellulose and low-concentrated samples). The appearance of an additional, high-temperature constituent in carbon oxide peaks at

high chromium concentrations suggests that another mechanism of CO_x formation may contribute to the total CO_x yield during cellulose pyrolytic degradation. With chromium increasing, the high-temperature component fraction of CO peak tended to increase for both series of the samples (Table 3). However, the proportion of a high-temperature component of CO_2 peak decreased insignificantly for impregnated samples but increased markedly for high-concentrated EA materials (Table 3).

For low-concentrated samples of both the series char yields are close to that of the original MCC and did not exceed 4-8 wt.% (Tables 1-2). But at chromium contents $>1.39\div3.64\cdot\cdot10^{-4}$ M Cr/1g MCC, an appreciable increase in char yield (up to 18-23 wt.%) was observed for both the DI and EA samples. It is generally accepted that cellulose pyrolysis follows two competing pathways. The first is via the formation of an intermediate product, levoglucosan, which further decomposes to various volatiles, and the second is a dehydration process which produces mostly char residue, water and carbon oxides [12]. Acidic additives can facilitate the second pathway of cellulose decomposition [4] because in the their presence dehydration processes are intensified [15]. For Mo-, V- and W-doped cellulose fibers a close relation was earlier established between char yields and the proportion of water in cellulose pyrolysis products; with the increase in water proportion, char yields tended to enhance [13]. These findings were explained by the acidic action of the additives studied. No such correlations are observed in the case of $(NH_4)_2Cr_2O_7$-modified MCCs (see Tables 1-2). Such a result is quite understandable because ammonium dichromate easily decomposes to Cr_2O_3 at relatively low temperatures (~280°C) [14]. Chromium (III) oxide, on the other hand, possesses rather weak acidic properties [15]. Hence, it should be another reason for increased char yields observed during pyrolysis of high-concentrated $(NH_4)_2Cr_2O_7$-doped MCCs and unusual thermal behavior of low-concentrated cellulosic materials. It is well known [16] that mechanism of adsorption of the chromium (VI), molybdenum (VI) and tungsten (VI) oxospecies during the impregnation of different supports is strongly influenced by the solution pH. For example, under neutral conditions Mo (VI) oxospecies are preferentially adsorbed in a monomeric form [17], while under more acidic situations polymerized species prevail in the adsorbed state [17-19]. Behavior of chromium (VI) ions is very close to that of molybdenum (VI) ions [16]. In aqueous solutions of ammonium dichromate the following equilibria exist:

$$Cr_2O_7^{2-} + H_2O \leftrightarrows 2HCrO_4^- \quad (1)$$

$$HCrO_4^- + H_2O \leftrightarrows CrO_4^{2-} + H_3O^+ \quad (2)$$

With decreasing chromium content, this equilibrium is shifted to the right, and monomeric CrO_4^{2-} ions are the most abundant species in very diluted solutions. On the contrary, in chromium-rich solutions di- and polychromates prevail. By analogy with the processes of chromium (VI) adsorption on alumina [16,19], we propose that when cellulose added to ammonium dichromate solution, the neutralization process of H_3O^+ ions with the surface cellulose hydroxyls may occur according to:

$$OH_{cel}^- + H_3O^+ \rightarrow 2H_2O \quad (3)$$

Table 3. High temperature component fractions in CO_x evolution peaks for the DI and EA samples

Sample	Chromium content $\cdot10^4$ (moles Cr per 1g MCC)	High-temperature fraction of CO_x peak (%)		Sample	Chromium content $\cdot10^4$ (moles Cr per 1g MCC)	High-temperature fraction of CO_x peak (%)	
		CO_2	CO			CO_2	CO
MCC	0.00	0.0	0.0	MCC	0.00	0.0	0.0
DI-1	$2.27\cdot10^{-1}$	0.0	0.0	EA-1	$2.20\cdot10^{-2}$	0.0	0.0
DI-2	$4.54\cdot10^{-1}$	0.0	0.0	EA-2	$1.07\cdot10^{-1}$	0.0	0.0
DI-3	3.64	32.4	48.4	EA-3	1.39	12.9	25.0
DI-4	7.27	28.1	46.7	EA-4	2.92	32.2	42.3
DI-5	14.54	20.6	60.6	EA-5	9.12	29.3	45.9

which shifts equilibria (1) and (2) to the right and leads to the anchorage of the Cr (VI) oxospecies in the monomeric form on the cellulose surface. As a result of such an anchoring, a chelated compound of chromium (VI) with cellulose hydroxy groups is formed. Chelated complexes of Mo (VI), W (VI), V (V), B (III) and some other ions with many organic hydroxy compounds (including carbohydrates) are known to easily be formed in aqueous solutions [20-22]. It is worth to note that such complexing is accompanied by consumption of H^+ ions, and, as a rule, mononuclear metal complexes are formed [20,21]. The lack of sufficient amounts of free H^+ (or H_3O^+) ions in diluted $(NH_4)_2Cr_2O_7$ solutions excludes the possibility of acid-catalyzed cellulose decomposition to

take place. On the other hand, formation of chelated complexes of Cr (VI) ions with cellulose hydroxy groups (including ester-like bonds crosslinking large fragments of cellulose structure) would enhance thermal stability of cellulose. Such processes are also characteristic for phosphate-modified cellulosic materials [23]. This explains the negative temperature shifts of H_2O, CO_2 and CO evolution peaks for low-concentrated $(NH_4)_2Cr_2O_7$-doped MCCs. With chromium increasing, di- and polychromate-ions prevail in ammonium dichromate solutions. Some excess of H^+ ions, therefore, is observed in high-concentrated solutions of $(NH_4)_2Cr_2O_7$. It may be supposed that this excess cannot be neutralized by complexing of chromate species with cellulose hydroxy groups. Then the adsorption of di- and polychromate species on the cellulose surface (without complexing) at high chromium concentrations is one of the possible reasons for the enhanced carbonizing effect of chromium in high-concentrated samples. The presence of condensed chromates in the cellulose samples facilitates the continuous generation of H^+ ions catalyzing cellulose dehydration processes.

Summarizing the above considerations, the observed differences in thermal behavior of low- and high-concentrated samples may be explained in terms of two forms of chromium species adsorbed on the surface of $(NH_4)_2Cr_2O_7$-doped cellulosics: (i) highly dispersed (possibly, CrO_4^{2-}exchanged) chromium species at low ammonium dichromate contents ($<1.39\div3.64\cdot10^{-4}$ M Cr/1g MCC) and (ii) polychromate species or a separate phase of $(NH_4)_2Cr_2O_7$ at higher chromium concentrations.

The presence of a separate phase of $(NH_4)_2Cr_2O_7$ in the sample with the highest chromium concentration ($3.03\cdot10^{-3}$ M Cr/1g MCC; EA series) has been confirmed by XRD analysis (Fig. 2, pattern 5).

Conclusions

Substantial differences in thermal behavior of low- and high-concentrated $(NH_4)_2Cr_2O_7$-doped microcrystalline cellulose materials (maximum temperatures and relative yields of evolved gases, character of CO_x evolution, char yields) have been established during their carbonization. These differences can be explained in terms of two forms of chromium species adsorbed on the surface of $(NH_4)_2Cr_2O_7$-doped cellulosics: (i) a highly dispersed (possibly, CrO_4^{2-}-exchanged) chromium species at low ammonium dichromate contents ($<1.39\cdot10^{-4}$ M Cr/1g MCC) and (ii) a separate phase of $(NH_4)_2Cr_2O_7$ at higher chromium concentrations. It is supposed that in the latter case, the interaction of more acidic di- and polychromate species with hydroxy groups of cellulose surface leads to the formation of H^+ ions facilitating the increased char yields during the cellulose pyrolysis.

References

1. Ermolenko IN, Lyubliner IP, Gulko NV. Chemically modified carbon fibers. Berlin (Germany): VCH Publications, 1990.
2. Friedel RA, Queiser JA and Retkofsky HL. Coial-like substances from low-temperature pyrolysis at very long reaction times. J. Phys. Chem. 1970;71(4):908-912.
3. Shafizadeh F. Introduction to pyrolysis of biomass. J. Anal. Appl. Pyrolysis 1982;3:283-305.
4. Shindo S, Nakanishi Y, Some Y. Carbon fibers from cellulose fibers. Appl. Polymer Symposia 1969;9:271-284.
5. Mack CH, Donaldson DJ. Effect of bases on the pyrolysis of cotton cellulose. Text. Res. J. 1967;37(12):1063-1071.
6. Dollimore D, Hoath MJ. The kinetics of the oxidative degradation of cellulose and cellulose doped with chlorides. Thermochim. Acta 1987;121:273-282.
7. Kurnevich GI, Loiko EV, Gert EV, Skoropanov AS, Bujanova VK, Gridina UF. Study of the influence of ammonium salts on the regenerated cellulose thermodestruction. Thermochim. Acta 1985;90(compl.):335-338.
8. Kotlyarova ES, Petrov IY, Pugachov VM, Patrakov YF, Kryazhev YG. Temperature-programmed pyrolysis of cellulose fibers doped with various inorganic additives. In: EUROCARBON'2000 (Ext. Abstr. 1st World Conf. on Carbon), Vol. 2, Berlin (Germany): 2000. p. 533-534.
9. Patrakov YF, Petrov IY, Kotlyarova ES and Kryazhev YG. Continuous analysis of gaseous products evolved during temperature-programmed pyrolysis of cellulose materials. In: EUROCARBON'98 (Ext. Abstr. Int. Conf. on Science and Technology of Carbon), Vol. 1, Strasbourg (France): 1998. p. 195-196.
10. Cellulose and cellulose derivatives (Ed. by N.M. Bikales and L. Segal). N.Y.: Wiley-Interscience. Part IV. 1971.
11. X-Ray Powder Diffraction File. ASTM. Joint Committee on Powder Diffraction Standarads, Philadelphia, Pa, 1973.
12. Liodakis SE, Statheropoulos MK, Tzamtzis NE, Pappa AA, Parissakis GK. The effect of salt and oxide-hydroxide additives on the pyrolysis of cellulose and *Pinus halepensis* pine needles. Thermochim. Acta 1996;278:99-108.
13. Kryazhev YuG, Petrov IYa, Khokhlova GP, Patrakov YuF. Transition Metal-Doped Carbon Fibrous Materials: Preparation, Characterization, and Dehydrogenation Activity. In: CARBON'97 (Ext. Abstr. 23rd Biennial Conf. on Carbon), Vol. 1, University Park, PennState (USA): 1997. p. 204-205.

14. Hesslop RB, Robinson PL. Inorganic Chemistry. 3rd edition. Amsterdam: Elsevier Publ. Co., 1967. p. 666.

15. Tanabe K. Solid acids and bases. N.y./London: Academic Press, 1970.

16. Iannibello A, Marengo S, Tittarelli P, Morelli G, Zecchina A. Spectroscopic study of the structure of chromium (VI), molybdenum (VI) and tungsten (VI) oxospecies anchored on aluminium oxide. J. Chem. Soc. Faraday Trans. Part I. 1984;80(8):2209-2223.

17. Jeziorowski H, Knözinger H. Raman and ultraviolet spectroscopic characterization of molybdena on alumina catalysts // J. Phys. Chem. 1979;83(9):1166-1173.

18. Wang L, Hall WK. On the genesis of molybdena-alumina catalyst. J. Catal. 1980;66(1):251-255.

19. Wang L, Hall WK. The preparation and genesis of molybdena-alumina and related catalyst systems. J. Catal. 1982;77(1):232-241.

20. Bartušek M. Chelation of metal anions with organic hydroxy compounds in water solutions. Folja přírodoved. fak. UJEP Brne 1984;25(6):1-66.

21. Bartušek M. Molybdate chelates with organic hydroxy compounds. Scr. fac. sci. natur. UJEP brun. 1983;83(3-4):107-115.

22. Bartušek M, Šustáćek V. Chelates of vanadium (V) with organic hydroxy compounds in aqueous solutions. Collect. Czech. Chem. Commun. 1983;48(10):2785-2797.

23. Jagtoyen M, Derbyshire F. Activated carbons from yellow poplar and white oak by H_3PO_4 activation. Carbon 1998;36(7-8):1085-1097.